Sensitivity and forced response analysis of anisotropy-mistuned bladed disks with nonlinear contact interfaces

Article (Accepted Version)

Sensitivity and Forced Response Analysis of Anisotropy-Mistuned Bladed Disks with Nonlinear Contact Interfaces

Adam Koscso

School of Engineering and Informatics
University of Sussex
Brighton, United Kingdom, BN1 9QT
Email: adam.koscso@sussex.ac.uk

E.P. Petrov

School of Engineering and Informatics
University of Sussex
Brighton, United Kingdom, BN1 9QT
Email: y.petrov@sussex.ac.uk

ABSTRACT

A new method has been developed for the analysis of nonlinear forced response of bladed disks mistuned by blade anisotropy scatter and for the forced response sensitivity to blade material anisotropy orientations. The approach allows for the calculation of bladed disks with nonlinear friction contact interfaces using the multi-harmonic balance method. The method uses efficient high-accuracy model reduction method for the minimization of the computational effort while providing required accuracy.

The capabilities of the developed methods are validated and demonstrated using a two-blade model. A thorough study of the influence of the material anisotropy mistuning and its sensitivity on the characteristics of the forced response is carried out using finite element modes of anisotropy mistuned realistic bladed disk with nonlinear friction joints of blade roots and shroud contacts. The dependency of the nonlinear forced

response on excitation level and contact pressure values has been carried out for anisotropy mistuned bladed disks.

INTRODUCTION

Blade mistuning is inevitable for practical bladed disk assemblies, due to the small imperfections in the manufacturing and assembly processes. It is known that the mistuning in bladed disk assemblies significantly increases the forced response levels compared to their tuned counterparts (e.g. see reviews in Refs. [1–4]). In order to withstand the extreme levels of temperature and pressure in the turbine stages of the modern gas turbine engines, the blades are made of directionally solidified and single crystal materials. The material of the single crystal blades is anisotropic and dynamic properties are dependent on the crystal orientation with respect to blade geometry shape. When bladed disks are assembled, blades with different crystal orientation result in a material-anisotropy-mistuned bladed disk.

One of the most important benefits of the application of single crystal blades is the extended fatigue life, which has been studied in e.g. [5] and in [6]. Due to the extended fatigue life monocrystalline blades are used for more and more gas-turbine applications. Therefore, it is useful to consider the mistuning coased by the variation in the crystal orientation of the monocrystalline blades.

Yet, there are only a few publications available that discuss the effect of the anisotropy angle variation on the static and dynamic responses.

The assessment of the contact stresses for the nonlinear forced response calculations are essential and it's variation on the root contact interfaces with changing crystal orientation have been studied by Savage in [7].

It is well known that the natural frequencies of the monocrystalline blades are influenced by the orientation of the single crystals. This has been investigated e.g. in [8] for turbine buckets using computational and experimental means and in [9] for simple beam models. The study of the sensitivity of the natural frequencies and mode shapes with respect to the crystal orientation parameters of bladed disks has been presented in [10], which shows significant sensitivities for the blade dominated and localized mode shapes.

The forced response of anisotropy mistuned bladed disks has been studied using reduced models in [11] and using high-fidelity reduction approach in [12].

In order to quantify the effect of anisotropy mistuning variation it is useful to calculate the sensitivity of system response with respect to the anisotropy orientation angles. Rajasekharan in [13] performed local and global sensitivity analysis to quantify the effect of anisotropy axis mistuning on static displacements due to centrifugal loading. The sensitivity of forced response of linear models of anisotropy mistuned bladed disk with respect to anisotropy angle parameters has been studied in [14].

The forced response of practical bladed disk assemblies consisting of several parts as blades, disk and underplatform dampers in many cases cannot be calculated with only linear models. In service, nonlinear forces occur on the friction contact interfaces, at blade root, shroud, underplatform dampers, etc., that make the forced response strongly

nonlinear. The friction joints introduced in the dynamic system are the main source of damping, therefore, it is necessary to assess the nonlinear forced to obtain correct excitation levels. Efficient calculation of the nonlinear forced response is carried out in frequency domain using the multiharmonic balance method [15–17]. A good review on the calculation of the nonlinear forced response with friction contact interfaces using the multiharmonic balance method can be found in [18].

In order to be able to calculate the nonlinear forced response of realistic bladed disk models with keeping the computation costs low, a model reduction method needs to be applied, e.g. [19, 20].

According to the authors knowledge, the sensitivity of the nonlinear forced response with respect to anisotropy orientation parameters is not yet available. Previous studies obtained sensitivities with respect to the contact interface characteristic of the nonlinear forced response and used them to obtain statistical properties or robustness in [21–23].

In this paper, a method for calculating the forced response and its sensitivities for anisotropy-mistuned bladed disks with nonlinear friction joints is presented. The modeling aspects of the method calculating the forced response and its sensitivities using the multiharmonic balance are explored. The sensitivities calculated with respect to the anisotropy angles defining the crystal orientation are validated using a realistic two-blade model. The influence of the different anisotropy mistuning patterns are studied for bladed disks with root contact and for bladed disks with root and shroud contacts. The dependency of the forced response and amplification factor on excitation levels and contact pressure values are studied. The sensitivity of the forced response is analyzed for varying crystal orientation of the two-blade model and for a material anisotropy mistuned bladed disk.

MODELING OF MATERIAL ANISOTROPY

The directionally solidified and single crystal blades used in the turbine stages of the modern gas turbines have anisotropic material properties. This results in a material that has direction dependent elastic constants. The stress-strain relationship for a linear-elastic material takes the form

$$\boldsymbol{\sigma} = \boldsymbol{C}\boldsymbol{\epsilon} \tag{1}$$

where, $\boldsymbol{\sigma}$ and $\boldsymbol{\epsilon}$ are the stress and strain tensors respectively in Voigt notation and $\boldsymbol{C}$ is the elasticity tensor. A general anisotropic material has 21 independent elastic parameters in the elasticity tensor $\boldsymbol{C}$. Nickel-base single crystal superalloys are often orthotropic materials and due to an additional symmetry in the crystal structure, it has only 3 independent elastic constants. These constants, defined in the coordinate system (CS) of material, are the shear modulus, the Young's modulus and the Poisson's ratio.

In order to carry out the finite element (FE) calculation, Eq. (1) has to be transformed from the local CS of the material to the global CS. In Fig. 1 the material CS is denoted with the axes $[001], [010]$ and $[001]$, the global CS is denoted with the axes X, Y and Z moreover, the blade CS is denoted with the axes x', y' and z'. The transformation

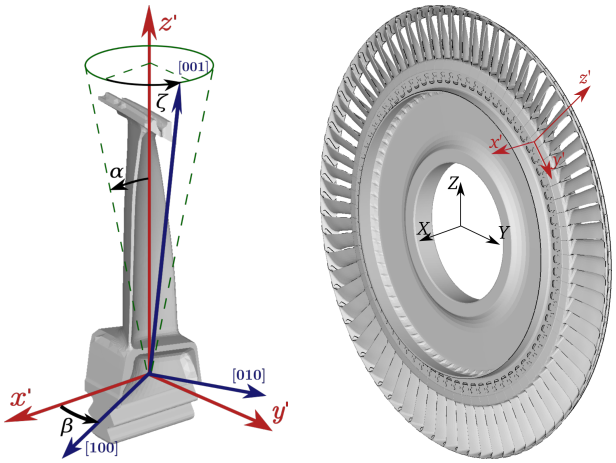

(a) Definition of the material and blade CS

(b) Blade CS in the global CS

Fig. 1: Definition of the material and blade coordinate system

of elasticity tensor $\boldsymbol{C}$ in Eq. (1) can be executed using the stress transformation matrix $\boldsymbol{T}$ as:

$$\boldsymbol{C}^*(\boldsymbol{R}_M, \boldsymbol{R}_B) = \boldsymbol{T}(\boldsymbol{R}_M, \boldsymbol{R}_B)\, \boldsymbol{C}\, \boldsymbol{T}^T(\boldsymbol{R}_M, \boldsymbol{R}_B) \tag{2}$$

The stress transformation matrix $\boldsymbol{T}$ is dependent on the rotation matrices $\boldsymbol{R}_M$ and $\boldsymbol{R}_B$. The rotation matrix $\boldsymbol{R}_M$ defines the coordinate transformation between the material CS and blade CS. This transformation can be described by anisotropy angles α, β and ζ depicted in Fig. $1a$. The primary anisotropy angle α defines the deviation of the $[001]$ material axis from the stacking axis z' of the blade. The secondary angle β shows the angle between axes $[100]$ and x'. The angle ζ defines the position of $[001]$ on polar coordinate basis. The rotation matrix $\boldsymbol{R}_B$ defines the position of the stacking axis z' of any blade with respect to the global Z axis.

It can be stated that the elasticity matrix $\boldsymbol{C}^*$ for each element in the FE model depends on the blade position in the assembly and on the anisotropy angles α, β and ζ. The element stiffness matrix is calculated using the element stiffness formulation for 3D isoparametric elements:

$$\boldsymbol{k}^e = \int_{V^e} \boldsymbol{B}^T\, \boldsymbol{C}^*\, \boldsymbol{B}\, dV \tag{3}$$

Where $\boldsymbol{k}^e$ is the FE stiffness matrix, $\boldsymbol{B}$ is the strain-displacement matrix and V^e is the volume of the element. The global FE stiffness matrix can be assembled with the standard global FE assembly process as:

$$\boldsymbol{K} = \bigcup_{j=1}^{N_e} \boldsymbol{k}_j^e \tag{4}$$

where N_e is the number of elements in the FE mesh.

SENSITIVITY CALCULATION OF MODAL PROPERTIES

First, in order to be able to calculate the sensitivity of the forced response of the dynamic system, the sensitivity of the modal characteristics has to be calculated.

In order to account for the geometric stiffening effects due to the centrifugal loading and for the frictional contact at joints, the nonlinear static calculation with friction contact interfaces is carried out.

$$\boldsymbol{K}_0(\boldsymbol{r})\boldsymbol{x}_0 + \boldsymbol{F}_{nln}(\boldsymbol{x}_0, \boldsymbol{r}) = \boldsymbol{F}_{ext} \tag{5}$$

where, $\boldsymbol{K}_0(\boldsymbol{r})$ is the linear stiffness matrix, $\boldsymbol{F}_{nln}(\boldsymbol{x}_0, \boldsymbol{r})$ is the vector of nonlinear internal forces, which includes the geometric nonlinearity and nonlinear contact effects, $\boldsymbol{x}_0$ is the vector of static displacements and $\boldsymbol{F}_{ext}$ is the vector of external forces that include centrifugal forces and static aerodynamic loading; $\boldsymbol{r}$ is the vector of anisotropy angles characterizing the orientation of material anisotropy axes (the total number of such angles for monocrystalline blades is $3 \cdot N_B$,where N_B is the number of blades in a bladed disk). For solution process of Eq. (5) the Newton-Raphson method is used in the open source FE software CalculiX [24].

The modal analysis of the bladed disk structure is carried out around the converged nonlinear static solution $\boldsymbol{x}_0$ and FE model of the bladed disk is changed by removing the friction contact pairs in order to free the nodes on the contact interface where the dynamic friction contact elements are applied. In order to avoid having rigid body modes, the disk and the blades are couple through multi-point constraints at four pair of nodes. These four pair of nodes are located at the root on the front and on the back surfaces, one of the node from the pair is on the blade and the other one is on the disk.

The eigenvalue problem of a multi-degree-freedom (MDOF) system is written as:

$$\boldsymbol{K}(\boldsymbol{r}, \boldsymbol{x}_0)\boldsymbol{\phi}_j = \lambda_j \boldsymbol{M}\boldsymbol{\phi}_j \tag{6}$$

where, $\boldsymbol{M}$ is the mass matrix and in the stiffness matrix $\boldsymbol{K}(\boldsymbol{r}, \boldsymbol{x}_0)$, the linear elastic stiffness matrix $\boldsymbol{K}_0(\boldsymbol{r})$, the stiffness contribution of the nonlinear internal forces $\partial \boldsymbol{F}_{nln}(\boldsymbol{x}_0, \boldsymbol{r})/\partial \boldsymbol{x}_0$ and the spin softening $\Omega^2 \boldsymbol{M}_\Omega$ are considered in the form:

$$\boldsymbol{K}(\boldsymbol{r}, \boldsymbol{x}_0) = \boldsymbol{K}_0(\boldsymbol{r}) + \frac{\partial \boldsymbol{F}_{nln}(\boldsymbol{x}_0, \boldsymbol{r})}{\partial \boldsymbol{x}_0} - \Omega^2 \boldsymbol{M}_\Omega \tag{7}$$

The eigenvalue and mode shape of mode number j are λ_j and $\boldsymbol{\phi}_j$. The stiffness matrix and the modal properties are dependent on the anisotropy orientation of the blade material. However, the mass matrix of the MDOF is generally independent of the crystal orientation of the blades. The sensitivity of eigenvalue λ_j is calculated by taking the derivative of Eq. (6) with respect to an anisotropy parameter r_k. For mass normalized mode shapes the sensitivity of

the eigenvalues results in [25]:

$$\frac{\partial \lambda_j}{\partial r_k} = \boldsymbol{\phi}_j^T \frac{\partial \boldsymbol{K}(\boldsymbol{r}, \boldsymbol{x}_0)}{\partial r_k} \boldsymbol{\phi}_j \tag{8}$$

The sensitivity of the mode shapes can be expanded over the mode shapes in the form:

$$\frac{\partial \boldsymbol{\phi}_j}{\partial r_k} = \sum_{k=1}^{m} c_{jk} \boldsymbol{\phi}_k + \boldsymbol{s}_j \tag{9}$$

where, the c_{jk} and $\boldsymbol{s}_j$ are the coefficients of the series expansion and the residual term accounting for the mode shapes not included in the summand respectively. For the detailed description of the calculation of the sensitivity of mode shapes the reader is referred to the earlier work of the authors [10].

For the calculation of the sensitivity of the modal characteristics the sensitivity of the stiffness matrix in Eq. (8) respect to the anisotropy angle is necessary. The sensitivities are calculated with open source FE software, CalculiX. The derivative of stiffness matrices are calculated on finite element level as

$$\frac{\partial \boldsymbol{k}^e}{\partial r_k} = \int\limits_{V^e} \boldsymbol{B}^T \frac{\partial \boldsymbol{C}^*}{\partial r_k} \boldsymbol{B} \, dV \tag{10}$$

NONLINEAR FORCED RESPONSE AND ITS SENSITIVITY CALCULATIONS

The equation for the forced vibrations of a material anisotropy mistuned bladed disk with nonlinear interactions at joints can be written in the form:

$$\boldsymbol{K}(\boldsymbol{r})\boldsymbol{x} + \boldsymbol{C}\dot{\boldsymbol{x}} + \boldsymbol{M}\ddot{\boldsymbol{x}} + \boldsymbol{f}(\boldsymbol{x}, \dot{\boldsymbol{x}}) = \boldsymbol{p}_0 + \boldsymbol{p}(t) \tag{11}$$

where $\boldsymbol{x}(t)$ is a vector of displacements for all degrees of freedom in the structure considered; $\boldsymbol{K}(\boldsymbol{r})$, $\boldsymbol{C}$ and $\boldsymbol{M}$ are structural stiffness, damping and mass matrices of FE model of a structure and $\boldsymbol{p}(t)$ is a vector of excitation forces; $\boldsymbol{r}$ is the vector of anisotropy angles characterizing the orientation of material anisotropy axes (the total number of such angles for monocrystalline blades is $3 * N_B$,where N_B is the number of blades in a bladed disk); $\boldsymbol{f}(\boldsymbol{x}, \dot{\boldsymbol{x}})$ is a vector of nonlinear contact interface forces which, for a case considered here, can be explicitly dependent on displacements, $\boldsymbol{x}$ and velocities, $\dot{\boldsymbol{x}}$ of the structural components. The contact forces occur in gas-turbine structures at the blade root joints of bladed discs, at contact surfaces of underplatform or tip dampers, at contact surfaces of adjacent interlock shrouds and at rubbing contacts between rotor and casing. The causes of nonlinear behavior are usually friction forces, unilateral interaction at the pairing contact surfaces, gaps, varying contact stiffness properties, as in the case of Hertzian contacts, etc. The static and dynamic external forces are represented here by terms $\boldsymbol{p}_0$ and $\boldsymbol{p}(t)$ respectively. The static loading is usually due to centrifugal forces or static component of aerodynamic forces and

the sources of dynamic excitation are, usually in bladed disks, the aerodynamic forces. A case of periodic excitation forces is considered, $\boldsymbol{p}(t) = \boldsymbol{p}(t + 2\pi/\omega)$, where ω is the principal excitation frequency. The forced response of a nonlinear structure under periodic excitation in majority of practical problems is also periodic. Because of this, the displacement of a structure can be represented by a restricted Fourier series

$$\boldsymbol{x}(t) = \boldsymbol{X}_0 + \sum_{j=1}^{n_x} \left(\boldsymbol{X}_j^c \cos k_j \omega t + \boldsymbol{X}_j^s \sin k_j \omega t \right) \tag{12}$$

where $\boldsymbol{X} = \left\{ \boldsymbol{X}_0, \boldsymbol{X}_1^c, ..., \boldsymbol{X}_{n_x}^s \right\}^T$ is vector of harmonic coefficients for displacements, n is the total number of harmonics used in the representation and k_j are the harmonic numbers. The equation of motion given by Eq.(11) can be solved efficiently in the frequency-domain. The number of harmonics used in the multiharmonic presentation can be chosen in order to achieve required accuracy of the calculation. The harmonic balance procedure applied to Eq. (11) provides the nonlinear equation of motion with respect to the vector of multiharmonic amplitudes, $\boldsymbol{X}$.

The FE models of mistuned bladed disk contain usually very large number of degrees of freedom (DOFs) which customarily have millions DOFs. The multiharmonic representation of the solutions allows avoidance the unpractical search of the solution in time-domain - when the time-consuming integration of equation has to be performed. However, the size of the frequency-domain equations increases significantly and to overcome this the effective model reduction techniques are applied for the high-fidelity analysis of vibrations. Following the approach in Ref. [26], the multiharmonic nonlinear equation of motion given by Eq. (11) is transformed to the form:

$$\boldsymbol{R} = \boldsymbol{X} - \widetilde{\boldsymbol{A}}(\omega, \boldsymbol{r}) \left(\boldsymbol{F}(\boldsymbol{X}) - \boldsymbol{P} \right) \tag{13}$$

where $\boldsymbol{X}$ is vector of multiharmonic amplitudes determined at the bladed disk nonlinear contact interface nodes, $\boldsymbol{P}$ is the multiharmonic vector of excitation forces; $\boldsymbol{F}(\boldsymbol{X})$ is the multiharmonic nonlinear contact forces; the multiharmonic forced response function (FRF) matrix, $\widetilde{\boldsymbol{A}}$, is expressed in the form through the FRF matrices of individual harmonics, $\boldsymbol{A}_{k_j}$:

$$\widetilde{\boldsymbol{A}}(\omega, \boldsymbol{r}) = diag \left(\boldsymbol{A}_0, \begin{bmatrix} \boldsymbol{A}_{k_1}^{\mathrm{Re}} & \boldsymbol{A}_{k_1}^{\mathrm{Im}} \\ -\boldsymbol{A}_{k_1}^{\mathrm{Im}} & \boldsymbol{A}_{k_1}^{\mathrm{Re}} \end{bmatrix}, ..., \begin{bmatrix} \boldsymbol{A}_{k_n}^{\mathrm{Re}} & \boldsymbol{A}_{k_n}^{\mathrm{Im}} \\ -\boldsymbol{A}_{k_n}^{\mathrm{Im}} & \boldsymbol{A}_{k_n}^{\mathrm{Re}} \end{bmatrix} \right) \tag{14}$$

The dynamic contact interface problem requires very accurate calculation of the FRF matrices and the high-accuracy reduction method developed in Ref. [19] allows the FRF matrix be represented as:

$$\boldsymbol{A}(\omega, \boldsymbol{r}) = \boldsymbol{A}^0(\boldsymbol{r}) + \boldsymbol{A}^d(\omega, \boldsymbol{r}) \tag{15}$$

where the first term, $\boldsymbol{A}^0(\boldsymbol{r})$, is the exact flexibility matrix calculated at the contact nodes from the whole FE model of a bladed disk at one frequency, ω_0.

The second, dynamic term, $\boldsymbol{A}^d(\omega, \boldsymbol{r})$, is expressed in the form:

$$\boldsymbol{A}^d(\omega, \boldsymbol{r}) = \sum_{j=1}^{n_m} c_j \boldsymbol{\phi}_j \boldsymbol{\phi}_j^T \tag{16}$$

Moreover, for the calculation of the nonlinear forced response sensitivity we have to calculate the sensitivity of FRF matrix with respect to each k-th component of the anisotropy vector, r_k. Each j-th column, $\boldsymbol{a}_j$, of matrix $\boldsymbol{A}^0(\boldsymbol{r})$ is obtained by solution of the following equation:

$$\left[\boldsymbol{K}(\boldsymbol{r}) - \omega_0^2 \boldsymbol{M}\right] \boldsymbol{a}_j = \boldsymbol{e}_j; \qquad j = 1, ..., n_c \tag{17}$$

and the sensitivity of this matrix to anisotropy angles is calculated from:

$$\left[\boldsymbol{K}(\boldsymbol{r}) - \omega_0^2 \boldsymbol{M}\right] \frac{\partial \boldsymbol{a}_j}{\partial r_k} = \frac{\partial \boldsymbol{K}(\boldsymbol{r})}{\partial r_k} \boldsymbol{a}_j; \qquad j = 1, ..., n_c \tag{18}$$

where n_c is the total number of contact DOFs.

The sensitivity of the dynamic term to the anisotropy angles:

$$\frac{\partial \boldsymbol{A}^d(\omega, \boldsymbol{r})}{\partial r_k} = \sum_{j=1}^{n_m} \frac{\partial c_j}{\partial r_k} \boldsymbol{\phi}_j \boldsymbol{\phi}_j^T + c_j \left(\frac{\partial \boldsymbol{\phi}_j}{\partial r_k} \boldsymbol{\phi}_j^T + \boldsymbol{\phi}_j \frac{\partial \boldsymbol{\phi}_j^T}{\partial r_k} \right) \tag{19}$$

where $c_j = \left(\omega^2 - \omega_0^2 - i\eta_j \omega_j^2\right) / \left[\left(\omega_j^2 - \omega_0^2\right)\left((1 + i\eta_j)\omega_j^2 - \omega^2\right)\right]$; ω_j, η_j and $\boldsymbol{\phi}_j$ are natural frequency, modal damping and mode shape; the derivative $\partial c_j / \partial r_k$ is calculated taking into account the dependency of the modal properties of the bladed disk on the anisotropy angles and obtaining the modal sensitivity properties as it is described in the previous section; n_m is the total number of modes used for the calculation of the dynamic FRF matrix component, $\boldsymbol{A}^d$.

Owing to the fact that the number of nonlinear DOFs in contact problems is much smaller (sometimes by several orders of magnitude) than the total number of degrees of freedom, the reduction of the model is straightforward. It is done by the calculation of the high accuracy FRF matrices for each of the harmonics only for nonlinear DOFs. The size of Eq. (13) is equal to the number of harmonic coefficients for nonlinear DOFs only.

The solution of Eq. (13) is performed by Newton-Raphson method with the solution continuation:

$$\boldsymbol{J}\left(\boldsymbol{X}^{(k)}\right)\left(\boldsymbol{X}^{(k+1)} - \boldsymbol{X}^{(k)}\right) = \boldsymbol{R}\left(\boldsymbol{X}^{(k)}\right) \tag{20}$$

where the Jacobian of the nonlinear equation $\boldsymbol{J} = \partial \boldsymbol{R} / \partial \boldsymbol{X}$ is calculated analytically (see Ref. [15]). The sensitivity of the found solution, $\boldsymbol{X}^*$, with respect to the material anisotropy angles are calculated from equation (12), which is obtained from Eq. (13) by differentiating it with respect to the material anisotropy vector, $\boldsymbol{r}$ and taking into account

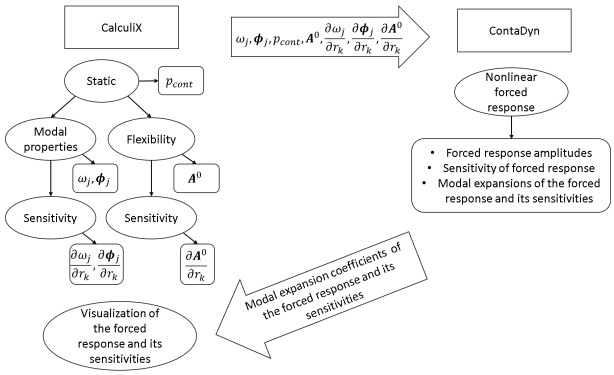

Fig. 2: Workflow of the nonlinear forced response calculation, version 1

explicit dependency of the FRF matrix on this vector:

$$\boldsymbol{J}\left(\boldsymbol{X}^*\right)\frac{\partial \boldsymbol{X}^*}{\partial \boldsymbol{r}} = \frac{\partial \boldsymbol{R}\left(\boldsymbol{X}^*\right)}{\partial \boldsymbol{r}} = \left[\frac{\partial \boldsymbol{A}^0}{\partial \boldsymbol{r}} + \frac{\partial \widetilde{\boldsymbol{A}}(\omega)}{\partial \boldsymbol{r}}\right]\left(\boldsymbol{F}\left(\boldsymbol{X}^*\right) - \boldsymbol{P}\right) \tag{21}$$

The workflow of the calculation of the nonlinear forced response with friction joints is depicted in Fig. 2. In the left hand side of the figure the processes carried out with CalculiX are shown. First, the static calculation of the bladed disk with nonlinear friction joints is performed under centrifugal loading. In order to calculate the contact forces for the nonlinear static FEM calculations the Coulomb law and unilateral interactions along normal direction was used. The pressure values obtained on the contact patches are used in the nonlinear forced response calculation for the assessment of the contact state.

In the second step, the modal properties, ω_j and $\boldsymbol{\phi}_j$, and the flexibility matrix $\boldsymbol{A}^0(\boldsymbol{r})$ are calculated around the found converged static solution. For this step, the contact definitions are removed for those nodes where the dynamic friction contact elements are planned to be applied. In order to avoid rigid body motion, the blades are constrained by a small number of single point constrains to the disk.

After the calculation of the modal properties and the flexibility matrix, their sensitivities with respect to the anisotropy angles $\partial\omega_j/\partial r_k, \partial\boldsymbol{\phi}_j/\partial r_k$ and $\partial\boldsymbol{A}^0(\boldsymbol{r})/\partial r_k$ are obtained, using the sensitivity module in CalculiX.

The data calculated with CalculiX are used as the input data of the nonlinear forced response analysis code ContaDyn. For the forced response calculation, only the nodal values calculated at the nonlinear contact nodes are necessary.

ContaDyn calculates the nonlinear forced response amplitudes, their sensitivities and the modal expansion of the forced response and its sensitivities. In the last step, the coefficients of the modal expansion together with the mode shapes are used for visualization of the forced response and its sensitivities over the full FE model of the mistuned bladed disk in the pre- and postprocessor of CalculiX: CalculiX GraphiX, if this is required.

MODELING ISSUES OF THE NONLINEAR FORCED RESPONSE

In order to efficiently calculate a high-fidelity model of a bladed disk the nonlinear forced response analysis must be computationally efficient while maintaining the high accuracy of the solution. To do this, a detailed analysis has been carried out using a pair of bladed disks, that consider the number of nonlinear nodes applied on the friction contact interfaces, selection of the harmonics, number of modes included and other modeling issues.

For the analysis of the number of modes and number of harmonics used, the model of two blades shown in Fig. 3a is used. The FE mesh of this model has ~ 14000 nodes. Centrifugal loading is applied and the nonlinear friction contact conditions are defined on the root and between the blade shrouds. Each sector has 6 contact interfaces, 4 at the root and 2 contact surfaces on the shroud. The simulation of the nonlinear forced response is carried out with a reduced number of nonlinear nodes on the contact interfaces compared to the number of nodes in the FE model. On each of the 4 root interfaces 12 nodes are distributed and on each of the shroud interfaces 3 nodes are used. The total number of nonlinear contact nodes is 102. The nonlinear nodes are uniformly distributed on the contact surfaces.

The material of the blades is single crystal superalloy and these two blades have different crystal orientation, therefore they are detuned. The harmonic loading of the dynamic model is applied at one node on each blade, in the middle of the leading edge, with a phase shift of 38.4°, which corresponds to engine order (EO) 8. The interfaces on the shrouds that are not in contact, are constrained so that only tangential displacements are allowed on these surfaces. The forced response is calculated at the midspan of the leading edge of the blade on the left hand side. On the frequency range of 3.95 and 4.3, the first resonance is for the mode shape when the two blades are vibrating in-phase and at the second resonance out-of-phase.

For the analysis of the number nonlinear contact nodes, the model shown in Fig. 3b is used. This model has the same geometry, however a finer mesh, which is necessary to study the convergence characteristic related to the number of discretization nodes. The finer mesh allows selecting nodes on the paired contact interfaces that have the same spatial coordinates. Centrifugal loading is applied and the nonlinear friction contact conditions are defined on the root and between the two blades on the shroud. The analysis is carried out with EO 8 and with two different excitation levels. The simulation with lower excitation amplitude results in free contact condition between the two shrouds, and by applying the higher excitation level, the shrouds come into contact. Using these two excitations levels, it can be assessed how many nonlinear nodes are required for analyses with free shrouds and with shrouds when nonlinear contact is modeled.

In Fig. 4, the dependency of the forced response on number of modes used for the forced response analysis is shown. The excitation frequency of the harmonic loading is normalized with the first natural frequency of the single blade. For this calculation, the first five harmonics are used in the analysis. The results show that good approximation of the solution can be achieved with 20-30 modes. For this model, with more modes used for the FRF matrix calculation, the resonance frequencies shift to lower values and the forced response magnitude increases.

One important aspect of the multiharmonic balance method is how many and which harmonic coefficients are used in the multiharmonic displacement expansion. Here, forced response calculations are carried out with: (i) only

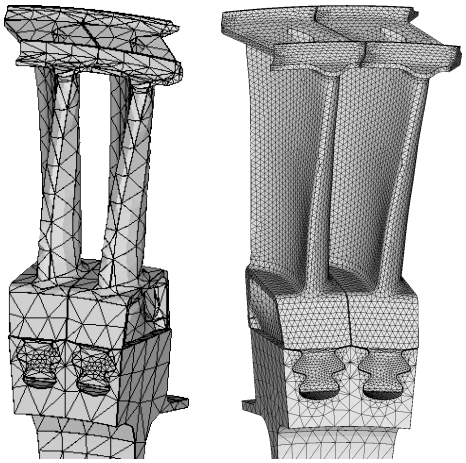

(a) Model 1 (b) Model 2

Fig. 3: Two-blade models

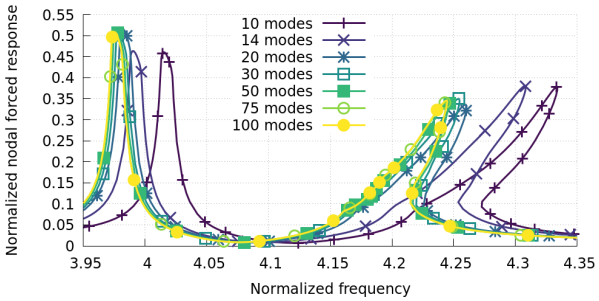

Fig. 4: Dependency of the forced response of blade 1 on the number of mode shapes

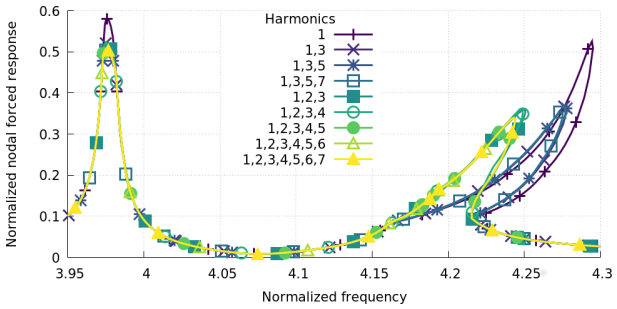

Fig. 5: Dependency of the forced response of blade 1 on the calculated harmonic coefficients

odd harmonics and with (ii) odd and even harmonics. For the FRF calculation the first 75 modes are included.

It is seen in Fig. 5 that the first nonlinear resonance peak can be calculated with harmonics 1 and 3 with sufficient accuracy. In order to calculate the second resonance peak both odd and even harmonics need to be included. Good results can be achieved with harmonics 1, 2 and 3, but for the fully converged solution, with respect to the frequency location of the resonance peaks and the maximum resonance amplitudes, according to the experiences obtained with numerical studies the calculation of the first five harmonics is sufficient, see Fig. 5.

The forced response with varying number of nonlinear nodes are shown in Fig 6a. In this figure, the nonlinear

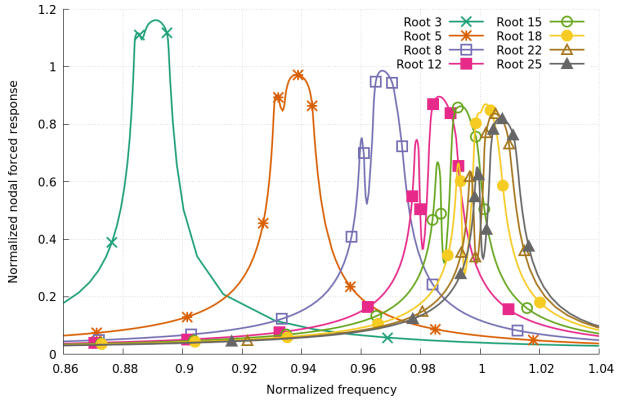

(a) Forced response with low excitation level

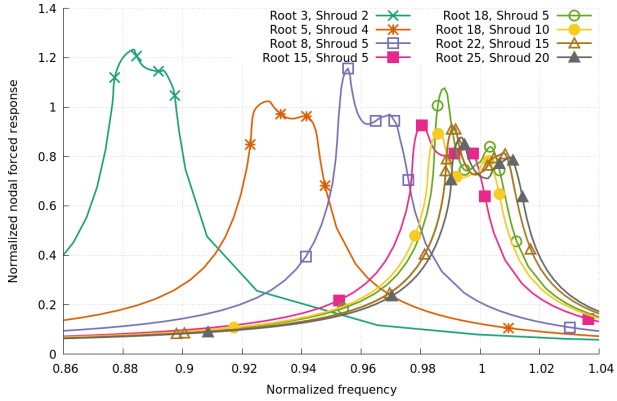

(b) Forced response with high excitation level

Fig. 6: Dependency of the forced response of blade 1 on number of nonlinear contact nodes

forced response of the blade 1 from the two blades is shown for the lower excitation level when the shroud contact interfaces do not come into contact. The number of nonlinear nodes on every root interface is changed from 3 to 18, which results in the change of total number of nonlinear nodes of from 24 to 200. With increase the number of nonlinear nodes, a tendency can be observed: the resonance frequency increases and the maximum forced response decreases. The difference between the forced response calculated with 18, 22 and 25 nonlinear nodes is small, therefore for the analysis of this system consisting of two blades, 18 nodes can be sufficient.

The excitation level can be increased such that the contact interfaces on the blade shrouds come into contact. This way the number of necessary nonlinear nodes on the shrouds can be assessed as well for this model. The forced response for this loading is shown in 6b. It is shown that for this model at least 10 nonlinear nodes should be applied on the shroud contact interfaces.

The studies performed here on the number of modes, number of harmonics included and number of nonlinear contact nodes demonstrate that sufficiently accurate nonlinear forced response can be achieved with appropriate choice of parameters.

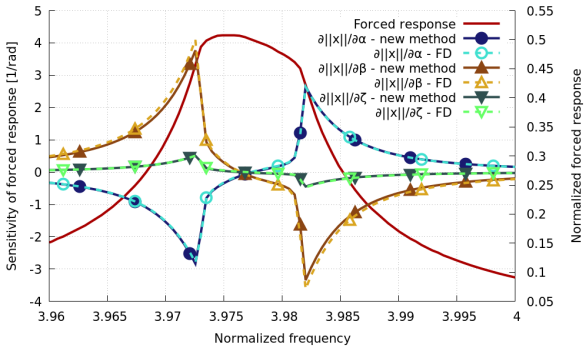

Fig. 7: Validation of the sensitivity of forced response

VALIDATION OF THE SENSITIVITY OF NONLINEAR FORCED RESPONSE

The calculation of the sensitivity of the forced response with respect to the anisotropy angles α, β and ζ has been carried out using the FE model shown in Fig. 3a. The boundary conditions and the static and dynamic loading are the same as described in the section before.

The sensitivities have been calculated using the new method, which calculates the sensitivities analytically, with respect to the three anisotropy angles of blade 1. These sensitivities are compared with sensitivity values approximated using the finite difference (FD) method. In order to do this the forced response has been calculated for two different orientations of blade 1. First, using the modal characteristics and flexibility matrix calculated for initial crystal orientation. Second, using modal properties and the flexibility matrix calculated for a FE model where one of the anisotropy angles r_k that define the crystal orientation is increased by a small value Δr_k. The sensitivity of the forced response is then approximated for each excitation frequency on the frequency range with the equation

$$\frac{\partial \boldsymbol{x}}{\partial r_k} \approx \frac{\boldsymbol{x}(r_k + \Delta r_k) - \boldsymbol{x}(r_k)}{\Delta r_k} \tag{22}$$

where, r_k can be α, β or ζ of blade 1.

In Fig. 7 an example of the forced response of blade 1 and its sensitivity with respect to the anisotropy angles α, β and ζ of the same blade are shown. The sensitivities calculated with the new method are shown by solid lines and the sensitivities obtained with the FD method are plotted by dashed lines. The results obtained with the two methods show a good agreement, for this and many other tests performed by the authors.

COMPARISON OF ANISOTROPY MISTUNING WITH FREQUENCY MISTUNING

Traditionally mistuned bladed disks were modeled with frequency mistuning that was introduced by adding lumped masses or by changes in the elasticity and shear modulus to change the natural frequency of the individual blades. In this section, the traditional method of modeling mistuning is compared to the anisotropy modeling used in this work.

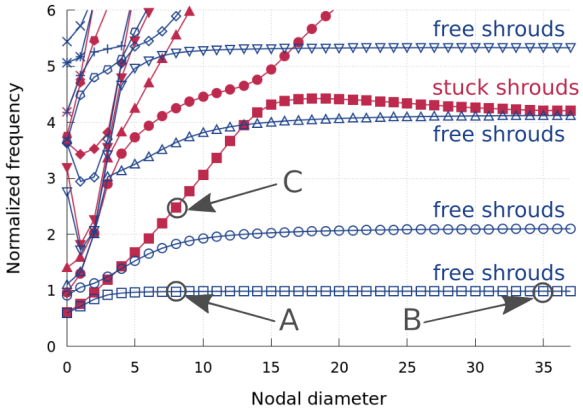

Fig. 8: Natural frequency-nodal diameter diagram of the cyclic symmetric model with stuck and free shroud interfaces

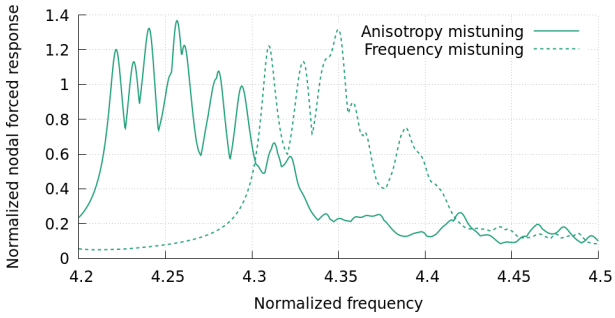

Fig. 9: Envelope of the linear forced response calculated with anisotropy and frequency mistuning

First, a random anisotropy mistuning pattern is created for all blades in the bladed disk. The first natural frequencies are calculated for all stand-alone blades with random crystal orientations and the nominal elasticity and shear modulus. Second, for all blades the Young's modulus and shear modulus is scaled while keeping the anisotropy angles constant for all blades at their mean value, so that the same stand-alone first natural frequencies are obtained. In the next step, the natural frequencies and mode shapes have been calculated for the frequency mistuned and for the anisotropy orientation mistuned bladed disk.

The linear forced response, considering stuck contact interfaces, has been calculated for engine order 35 excitation for the first mode family, marked by D in Fig. 8. The forced response has been obtained for bladed disks with anisotropy and frequency mistuning. One example of our studies in Fig. 9, showing the envelope of the forced response, shows that there is a deviation in the resonance frequency of bladed disks and that the envelope of the forced response show different behavior when it is modeled with frequency mistuning compared or with anisotropy mistuning.

Our studies show that it is essential to model the anisotropy mistuning directly, by assigning varying crystal orientation each blade. The difference in the nonlinear forced response is expected to be more significant, as this investigation excluded the deviation in the nonlinear contact stresses between the two modeling strategies.

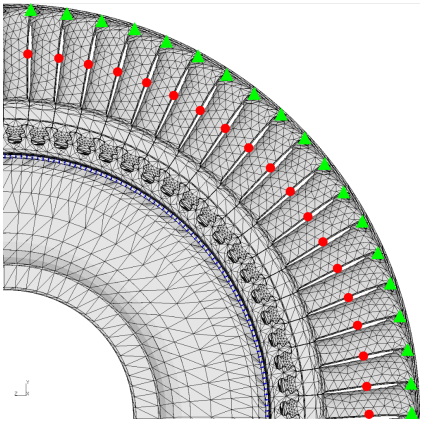

Fig. 10: Quarter of a bladed disk

ANALYSIS OF THE NONLINEAR FORCED RESPONSE OF BLADED DISKS

The analysis of the nonlinear forced response is performed with a full model of anisotropy-mistuned bladed disk consisting of 75 blades. The FE model of the bladed disk contains ~ 0.5 million nodes. The reduced model of the nonlinear forced response analysis contains 6 nonlinear nodes on each root interface and 4 nonlinear nodes on each shroud contact interface. For each blade sector there are 4 contact patches on the root and 2 on the shrouds, therefore the total number of nonlinear nodes is 1800 for the model with root contact only, and 2400 for the model with root and shroud contact respectively. The number of nodes used per sector for the calculation of the nonlinear forced response of the bladed disk is less than what is necessary to achieve a fully converged solution. This a compromise in order to keep computational expenses relatively low, while obtaining sufficiently accurate results. The nodal forced response values are calculated for the model with free shroud at the tip of the blade on the trailing edge, and for the model contact on both roots and shrouds at the midspan of the trailing edge. These nodes are shown in Fig. 10 at the tip of the blade with green triangles and at the midspand of the trailing edge with red circles. For the multiharmonic balance method the harmonic coefficients 1 and 3 are calculated and 500 mode shapes are used.

The statistical distribution for anisotropy angles α, β and ζ has been provided by the manufacturer of the blades. This distribution is not shared in this work due to confidentiality reasons.

The static contact pressures used in the nonlinear forced response calculation have been obtained using the anisotropy-mistuned bladed disk model. Because of this there is a scatter in the contact pressure values from blade to blade. The modal properties are also mistuned due to the anisotropy scatter. Therefore, in this work the effects of the anisotropy mistuning on the contact pressure values and modal characteristic are analyzed together in the nonlinear forced response calculation.

The natural frequency of the cyclic symmetric model has been calculated for all possible 37 values of nodal diameters. For the considered bladed disk, this calculation was done using the linear model of the blade sector. In this modal analysis, the fully stuck contact interfaces at blade roots were modeled by multiple point constraints. Two different contact conditions were considered for shrouds: (i) free shrouds (ii) stuck shrouds. In Fig. 8 the calculated

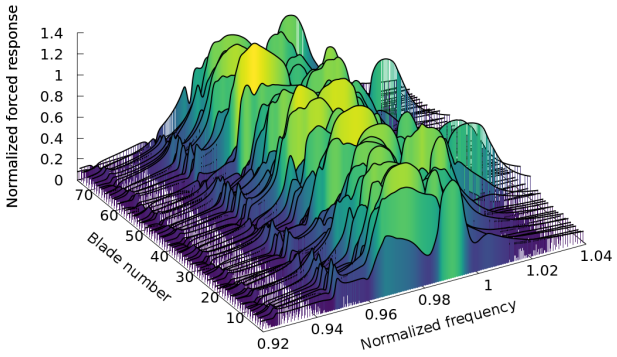

Fig. 11: Forced response of all blades of the mistuned bladed disk with pattern 1 using excitation level $||\boldsymbol{p}|| = 1$ for excitation frequency A

natural frequencies are shown. In this plot, the natural frequencies of the model where shrouds are free is shown with empty symbols and the natural frequencies of the model with stuck shrouds are shown with filled symbols. The frequency ranges and nodal diameters used for the harmonic excitation are shown as A, B and C.

Mistuned Bladed Disk without Shroud Contact

First, the forced response of the bladed disk is analyzed for a model where the nonlinear contact interfaces are only considered on the root and the shrouds are free. Using this model the effect of the root damping can be assessed for the anisotropy mistuned bladed disks. The periodical excitation forces are applied on the pressure side of each blade equally distributed over 8 nodes. In this work the amplitude of the normalized harmonic loading is changed between the values of 0.2, 0.6 and 1.

For the analysis, five different anisotropy mistuning patterns are generated using the realistic statistical distributions defined for each of the anisotropy angles the anisotropy angles α, β and ζ. For each blade in the bladed disk a set of 3 random anisotropy angles is generated. In order to assess the amplification factors due to mistuning, the forced response of a tuned bladed disk is also calculated. For this model all anisotropy angles are zero, $\alpha = \beta = \zeta = 0$, meaning the stacking axis is coinciding with the $[001]$ material axis.

The influence of different anisotropy mistuning patterns and different loading amplitude on the nonlinear forced response were analyzed for EO8 excitation that excites the first family of modes, denoted with A in Fig. 8

The forced response of all the blades is shown for mistuning pattern 1 in Fig. 11. This figure shown different maximum forced response magnitude for each blade over the frequency range. The maximum forced response of all the blades for each frequency, the envelope of the response, is shown in Fig.12 for bladed disks with 5 mistuned patterns. The mistuned bladed disks have higher resonance frequency and amplification factor compared to the tuned bladed disk response. The maximum amplification factor for every mistuning pattern is different for each loading conditions. Moreover, the maximum amplification factors are the highest for the smallest loading, which means, for the excitation level $||\boldsymbol{p}|| = 0.2$ the root damping is not significant.

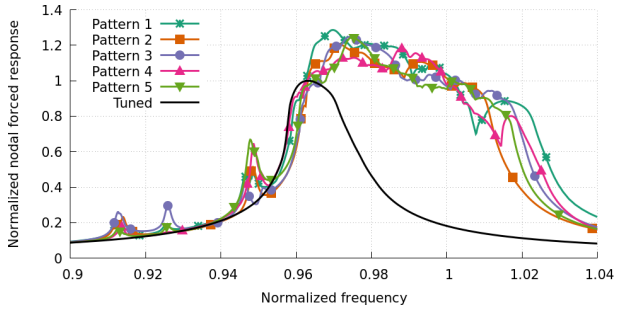

(a) $||\boldsymbol{p}|| = 1$

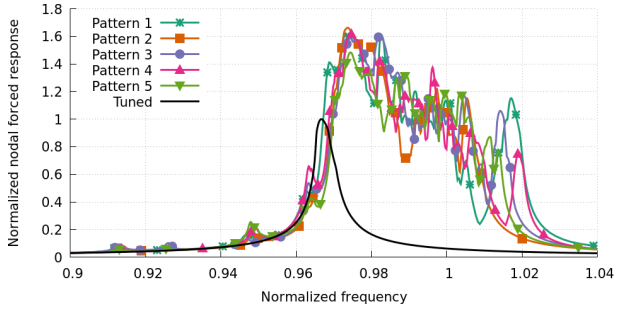

(b) $||\boldsymbol{p}|| = 0.2$

Fig. 12: Maximum forced response amplitude of anisotropy-mistuning bladed disk for excitation frequency A

Table 1: Mean of amplification factors

	$\|\|p\|\| = 1$	$\|\|p\|\| = 0.6$	$\|\|p\|\| = 0.2$
EO8	1.23	1.24	1.63
EO35	1.28	1.36	1.68

It has been investigated how the maximum forced response for each blade changes with the excitation level variation. In Fig. 13 the maximum forced response is shown for each blade over the frequency range 0.9-1.04. The plots show the results for the anisotropy mistuning pattern 1 and for the three excitation amplitudes. The similarity between the maximum forced response values for all the blades can be seen for $||\boldsymbol{p}|| = 1$ and $||\boldsymbol{p}|| = 0.6$, but the blades have significantly different maximum response for the excitation level $||\boldsymbol{p}|| = 0.2$. It can be seen that the excitation level influences the maximum blade response distribution.

The forced response of the tuned bladed disks, shown in Fig. 14, have been assessed for tuned bladed disks for EO8 and EO35 excitations with different excitation levels. It can be seen that the maximum response is not linear proportional to the magnitude of the harmonic excitation. This is due to the increased damping introduced to the dynamic system at the friction contact interfaces on the root. It is also visible that for the EO35, the maximum tuned response is lower than for EO8.

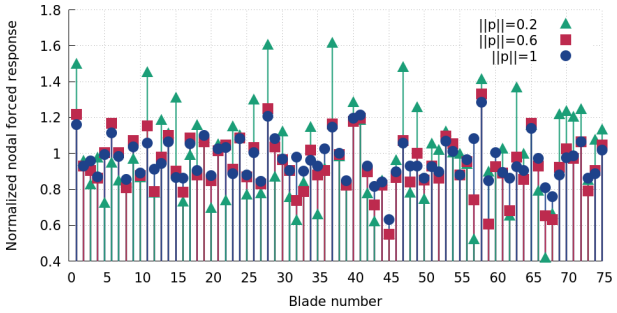

Fig. 13: Blade maximum forced response distribution with different loading conditions for excitation frequency A

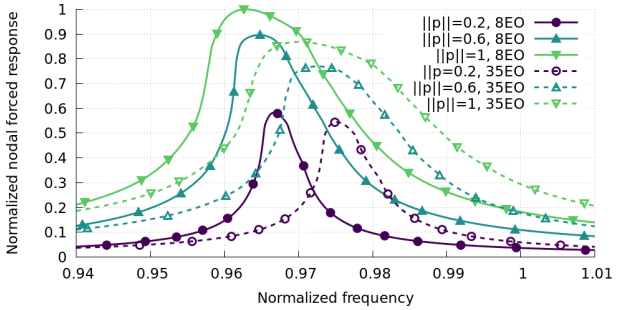

Fig. 14: Forced response calculated for tuned bladed disks with excitation A and B and with different excitation amplitudes

The nonlinear forced response of the bladed disks for the same mistuning patterns were calculated for EO35. The mean value of the maximum amplification factor for the five different mistuning patterns are shown in Table. 1 for EO8, EO35 and for the normalized excitation levels 0.2, 0.6 and 1.

Study of the separate and combined effect of contact pressure and modal anisotropy mistuning

The mistuning for the nonlinear forced response analysis originates from the variation of the contact pressure values from blade to blade and from the anisotropy mistuning of the modal characteristics. The pressure values on the contact interfaces are obtained for the mistuned bladed disk in the static calculation, which is called here static mistuning. The mistuning introduced with the natural frequencies, mode shapes and flexibility matrix are called here modal mistuning.

In order to quantify the effect of the mistuning on the nonlinear forced response due to the anisotropy mistuning only, analyses were performed using the contact pressure values calculated with the tuned bladed disk model. In Fig. 15 the envelope of the forced response is shown for two mistuning patterns, pattern 6 and 7 and for the excitation frequency B, see Fig. 8. For both mistuning patterns a simulation is performed with mistuned modal characteristic and with both modal and static mistuning. When only the modal mistuning is applied, the pressure values calculated for a tuned bladed disk are used.

It is clearly visible from Fig. 15, that the frequency of the highest response is different for the modal and for the

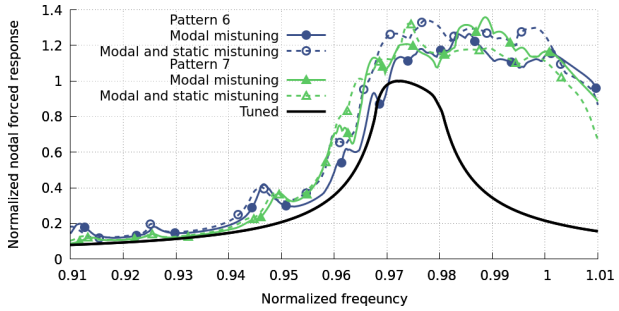

Fig. 15: Maximum nonlinear forced response with separate and combined mistuning effects for excitation frequency B

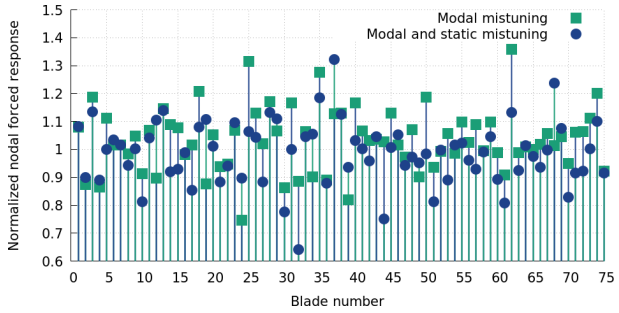

Fig. 16: Blade maximum forced response distribution with separate and combine mistuning effects for excitation frequency B and pattern 7

full mistuned bladed disk. For mistuning pattern 6 the maximum mistuning of the fully mistuned bladed disk is higher by 6.5%, but for mistuning pattern 7 the maximum amplification factor of the fully mistuned bladed disk resulted in 3% lower value compared to the model where only modal mistuning was introduced.

As described earlier the envelope of the is very similar for the modal mistuning and for modal and static mistuning. In order to see the difference between the difference between the forced response calculated with the two modeling methods, the maximum forced response distribution for all the blades are shown In Fig. 16 for pattern 7. In this figure it can be seen that the maximum amplitude of the blades significantly differ if the mistuning is only introduced in the modal characteristics or in the static pressure values as well.

Our study showed, accounting for the mistuning of the static pressure values is essential for the accurate calculation of the forced response. If only the modal mistuning is considered, there is an error in the maximum forced response amplitude and resonance frequency. Accounting for the combined effect of modal and static mistuning is essential for obtaining correct distribution of the maximum forced response amplitude distribution along the blades.

Mistuned Bladed Disk Model with Shroud Contact

The forced response of the mistuned bladed disk with root and shroud friction contact has been calculated. An example of the envelope of the forced response of 5 different mistuning patterns is shown in Fig. 17. It is visible

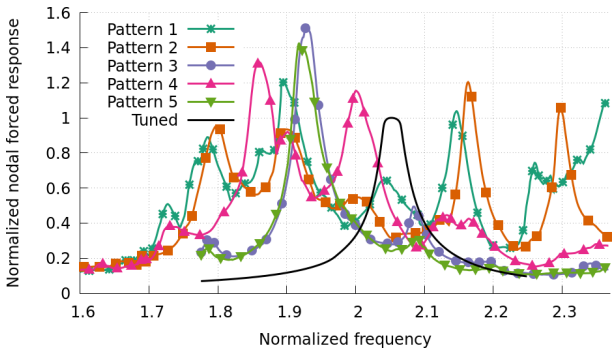

Fig. 17: Maximum forced response for mistuned blade disk with shroud contact for excitation frequency C

that different mistuning patterns can split the resonance peaks to different extent. For example the splitting of the resonances are significant for pattern 1,2 and 3 however negligible for pattern 3 and 5. The maximum amplification factors vary between 1.2 and 1.55 depending on the mistuning pattern.

ANALYSIS OF THE SENSITIVITY OF NONLINEAR FORCED RESPONSE

Two-blade model

The effect of variation of the material anisotropy orientation on the forced response have been studied for the model consisting of two anisotropy mistuned blades, shown in Fig. 3b. For this analysis the anisotropy angle α of blade 1 has been gradually increased from α_1 to α_{10} within the realistic range of this angle variation, while the other anisotropy angles are kept constant. This way it can easily be understood how influential the change of crystal orientation is on the nonlinear forced response and how the sensitivities reflect that. On the root interfaces 18 and on the shroud interfaces 10 nonlinear nodes are applied for the forced response analysis, which is 164 nonlinear nodes in total.

The forced response of blade 1 is obtained at the midspan of the trailing edge and shown in Fig. 18a. The response with the primary angle α_1 shows two resonance peaks. By increasing the primary anisotropy angle, the first resonance peak reduces and the second resonance peak increases. The frequency of both resonance peaks increase with higher values of α.

In Fig. 18b the sensitivity of the forced response of the first blade is shown for the different primary anisotropy angle crystal orientations. The reduction of the first resonance peak by increase of α is visualized by the negative sensitivities for α_3-α_8. The sensitivities show the shift of the second resonance peak by the negative sensitivities before and positive sensitivities after the resonance peak. The increase in amplitude for this resonance peak can be seen in the sensitivities as the sensitivity is positive at the frequency of the resonance peak.

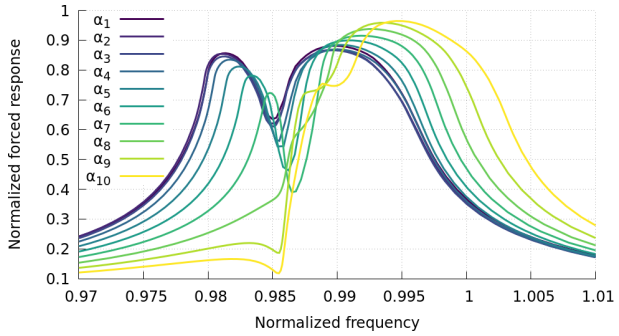

(a) Forced response

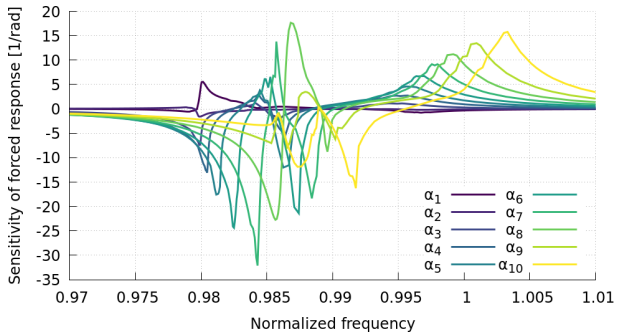

(b) Sensitivity of forced response

Fig. 18: Forced response and its sensitivity of blade 1 with varying α anisotropy angle

Bladed disk model

The sensitivity of the forced response has been calculated for the anisotropy mistuned bladed disk with pattern 1. In the calculation, the contact interfaces on the shrouds are not included, they are considered to be free. The forced response of a few selected blades that have high displacement magnitude are shown in Fig. 19.

Because the primary anisotropy angles α are the most influential on the forced response, the sensitivities are calculated with respect to these anisotropy angles of 4 different blades. Two of them have high displacements on this frequency range (blade number 37 and 58) and two of them have lower amplification than 1 (blade number 13 and 25). The sensitivities of the forced response are calculated at two blades that have high displacements, these are blade number 58 and 28. In Fig. 20a the sensitivities of the displacement at the midspan of the blade 58 is shown with respect to the primary anisotropy angle α of selected blades. The sensitivities are only significant with respect blade 13 and 28. The sensitivity with respect to the α of blade 28 is large at the frequency of the maximum forced response amplitude of blade 58 at $\omega = 0.97$, therefore the crystal orientation of this blade can influence the maximum amplification factor of the bladed disk. The sensitivity of the forced response of this blade is higher with respect to the α anisotropy angle of blade 13, but at this frequency the response is low.

The sensitivities of the nonlinear forced response of blade 28 with respect to the selected primary anisotropy angles are shown in Fig. 20b, that has high amplitudes at $\omega = 0.98$. The sensitivity with respect to this blade show

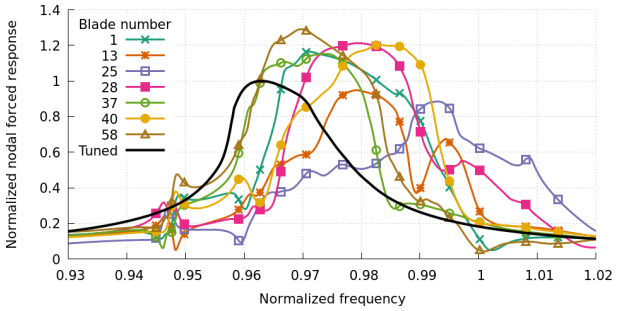

Fig. 19: Forced response of selected blades for mistuned blade disk for excitation frequency A

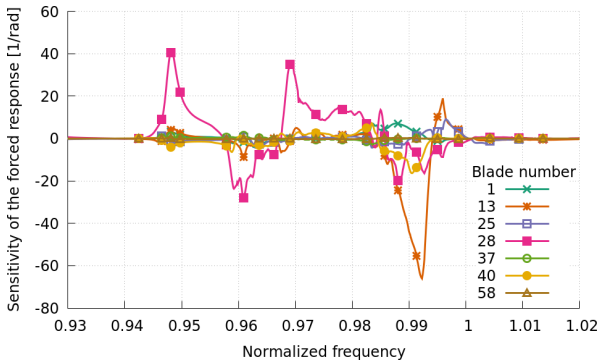

(a) Sensitivity of the forced response of blade 58

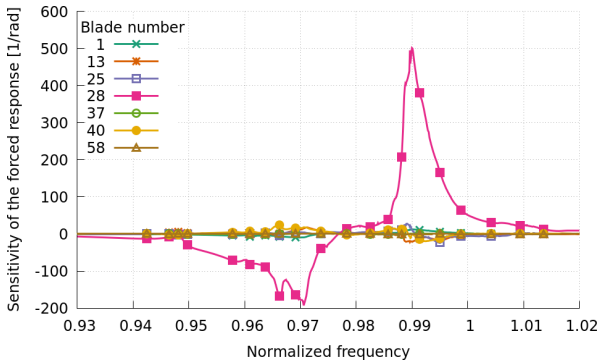

(b) Sensitivity of the forced response of blade 28

Fig. 20: Sensitivity of forced response of two blades with respect to α anisotropy angle of selected blades for excitation frequency A

positive value at the $\omega = 0.98$, moreover the sensitivity has the maximum value at 0.99 and the minimum value 0.9. This indicates, that with the increase of α primary angle of blade 28 the frequency of the maximum response displacement will shift to higher frequencies.

CONCLUSIONS

A method has been developed for the calculation of the nonlinear forced response of the anisotropy-mistuned bladed disks using high-fidelity models. The method uses the multiharmonic balance approach and the high-accuracy model reduction and the analytical formulation of all matrices in the nonlinear calculation for structures with friction joints. The method is capable of the calculation of the sensitivity of the forced response with respect to the material anisotropy angles of the single crystal blades.

The modeling aspects of the methodology for calculation of nonlinear forced response of realistic bladed disk models have been studied using a model with a pair of blades and a realistic mistuned bladed disk. The calculation of the sensitivity of the nonlinear forced response has been validated with the finite difference approximations. The necessity of the realistic modeling of anisotropy angles has been shown in comparison between frequency mistuning and direct anisotropy orientation mistuning.

The influence of the different anisotropy mistuning patterns has been demonstrated for bladed disk models with free shrouds and with shrouds that are in contact. The effects of the excitation level have been assessed on blade maximum forced response amplitudes. The separate and combined effect of contact pressure mistuning and material anisotropy mistuning has been studied for mistuned bladed disk models with nonlinear root contact interfaces. The sensitivity of the forced response with respect to anisotropy angles has been studied for a two-blade system and for a full mistuned bladed disk.

ACKNOWLEDGEMENTS

The authors are grateful for MTU Aero Engines AG for their financial support provided for this project and for the permission to publish this work.

REFERENCES

[1] Ewins, D. J., 1973. "Vibration characteristics of bladed disc assemblies". *Journal of Mechanical Engineering Science,* ***15***(3), pp. 165–186.

[2] Ewins, D. J., 1991. "The Effects of Blade Mistuning on Vibration Response - A Survey". In IFToMM Fourth International Conference on Rotordynamics. Prague, Czech Republic.

[3] Slater, J. C., Minkiewicz, G. R., and Blair, A. J., 1999. "Forced response of bladed disk assemblies - a survey". *The Shock and Vibration Digest*, Jan.

[4] Castanier, M., and Pierre, C., 2006. "Modeling and analysis of mistuned bladed disk vibration: Status and emerging directions". *Journal of Propulsion and Power,* ***22***(2), pp. 384–396.

[5] Arakere, N., and Swanson, G., 2002. "Effect of crystal orientation on fatigue failure of single crystal nickel base turbine blade superalloys". *Journal of Engineering for Gas Turbines and Power,* ***124***(1), pp. 161–176.

[6] Weiss, T., Voigt, M., Schlums, H., Mcke, R., Becker, K.-H., and Vogeler, K., 2009. "Probabilistic finite-element analyses on turbine blades". In Proceedings of the ASME Turbo Expo, Vol. 6.

[7] Savage, M. W. R., 2011. "The Influence of Crystal Orientation on the Elastic Stresses of a Single Crystal Nickel-Based Turbine Blade". *Journal of Engineering for Gas Turbines and Power,* ***134***(1), Oct., pp. 012501–012501–7.

[8] Manetti, M., Giovannetti, I., Pieroni, N., Horculescu, H., Peano, G., Zonfrillo, G., and Giannozzi, M., 2009. "The dynamic influence of crystal orientation on a second generation single crystal material for turbine buckets". In Proceedings of the ASME Turbo Expo, Vol. 6, pp. 125–133.

[9] Kaneko, Y., 2011. "Study on vibration characteristics of single crystal blade and directionally solidified blade". In Proceedings of the ASME Turbo Expo, Vol. 6, pp. 931–940.

[10] Koscso, A., Dhondt, G., and Petrov, E., 2018. "High-fidelity sensitivity analysis of modal properties of mistuned bladed disks regarding material anisotropy". In Proceedings of the ASME Turbo Expo, Vol. 7C.

[11] Kaneko, Y., Mori, K., and Ooyama, H., 2015. "Resonant response and random response analysis of mistuned bladed disk consisting of directionally solidified blade". In Proceedings of the ASME Turbo Expo, Vol. 7B.

[12] Zang, C., Tan, Y., and Petrov, E., 2018. "Analysis of forced response for bladed disks mistuned by material anisotropy orientation scatters". *Journal of Engineering for Gas Turbines and Power,* ***140***(2).

[13] Rajasekharan, R., and Petrov, E., 2018. "Analysis of deformation of mistuned bladed disks with friction and random crystal anisotropy orientation using gradient-based polynomial chaos expansion". In Proceedings of the ASME Turbo Expo, Vol. 7C.

[14] Koscso, A., Rajasekharan, R., and Petrov, E. P., 2018. "Sensitivity and uncertainity of modal characteristics and forced response of bladed disks mistuned by material anisotropy". In Proceedings of the 15th ISUAAAT, Oxford, UK. Paper No. ISUAAAT15-092.

[15] Petrov, E. P., and Ewins, D. J., 2003. "Analytical Formulation of Friction Interface Elements for Analysis of Nonlinear Multi-Harmonic Vibrations of Bladed Disks". *Journal of Turbomachinery,* ***125***(2), Apr., pp. 364–371.

[16] Laxalde, D., Thouverez, F., Sinou, J.-J., and Lombard, J.-P., 2007. "Qualitative analysis of forced response of blisks with friction ring dampers". *European Journal of Mechanics - A/Solids,* ***26***(4), July, pp. 676–687.

[17] Firrone, C., Zucca, S., and Gola, M., 2011. "The effect of underplatform dampers on the forced response of bladed disks by a coupled static/dynamic harmonic balance method". *International Journal of Non-Linear Mechanics,* ***46***(2), pp. 363–375.

[18] Krack, M., Salles, L., and Thouverez, F., 2017. "Vibration prediction of bladed disks coupled by friction joints". *Archives of Computational Methods in Engineering,* ***24***(3), pp. 589–636.

[19] Petrov, E., 2011. "A high-accuracy model reduction for analysis of nonlinear vibrations in structures with contact interfaces". *Journal of Engineering for Gas Turbines and Power,* ***133***(10).

[20] Krack, M., Scheidt, L.-V., Wallaschek, J., Siewert, C., and Hartung, A., 2013. "Reduced order modeling based on complex nonlinear modal analysis and its application to bladed disks with shroud contact". In Proceedings of

the ASME Turbo Expo, Vol. 7 B.

[21] Petrov, E. P., 2008. "A Sensitivity-Based Method for Direct Stochastic Analysis of Nonlinear Forced Response for Bladed Disks With Friction Interfaces". *Journal of Engineering for Gas Turbines and Power,* ***130***(2), Feb., pp. 022503–022503–9.

[22] Petrov, E., 2009. "Method for sensitivity analysis of resonance forced response of bladed disks with nonlinear contact interfaces". *Journal of Engineering for Gas Turbines and Power,* ***131***(2).

[23] Krack, M., Panning, L., Wallaschek, J., Siewert, C., and Hartung, A., 2012. "Robust design of friction interfaces of bladed disks with respect to parameter uncertainties". In Proceedings of the ASME Turbo Expo, Vol. 7, pp. 1193–1204.

[24] Dhondt, G., 2004. *The Finite Element Method for Three-Dimensional Thermomechanical Applications*. John Wiley & Sons, Chichester, England, UK.

[25] Adelman, H., and Haftka, R., 1986. "Sensitivity analysis of discrete structural systems". *AIAA Journal,* ***24***(5), pp. 823–832.

[26] Petrov, E. P., and Ewins, D. J., 2005. "Method for Analysis of Nonlinear Multiharmonic Vibrations of Mistuned Bladed Disks With Scatter of Contact Interface Characteristics". *Journal of Turbomachinery,* ***127***(1), Feb., pp. 128–136.